VERSITA

Acta Geophysica
vol. 57, no. 4, pp. 950-980
DOI: 10.2478/s11600-009-0026-5

Nocturnal Low-Level Jet over a Shallow Slope

Alan SHAPIRO and Evgeni FEDOROVICH

School of Meteorology, University of Oklahoma, Norman, USA
e-mails: ashapiro@ou.edu (corresponding author), fedorovich@ou.edu

Abstract

A simple theory is presented for a nocturnal low-level jet (LLJ) over a planar slope. The theory extends the classical inviscid inertial-oscillation model of LLJs to include up- and downslope motion in the boundary layer within a stably stratified environment. The particular scenario considered is typical of LLJs over the Great Plains of the United States: southerly geostrophic wind over terrain that gently slopes down toward the east. First, an initial value problem for the coupled equations of motion and thermodynamic energy is solved for air parcels suddenly freed of a frictional constraint near sunset. The solution is an oscillation that takes, on the hodograph plane, the form of an ellipse having an eastward-oriented major axis and an eccentricity that increases with increasing stratification and slope angle. Next, the notion of a tilted residual layer (TRL) is introduced and used to relate initial (sunset) air parcel buoyancy to free-atmosphere stratification and thermal structure of the boundary layer. Application of the TRL-estimated initial buoyancy in the solution of the initial value problem leads to expressions for peak jet strength and the slope angle that maximizes the jet strength. Analytical results are in reasonable qualitative agreement with observational data.

Key words: low-level jet, inertial oscillation, planar slope, stable stratification, residual layer.

1. INTRODUCTION

The nocturnal low-level jet (LLJ), also known as the southerly low-level jet, is a warm-season boundary-layer phenomenon that commonly occurs over the Great Plains of the United States and other places worldwide, typically in

regions east of mountain ranges or in the vicinity of strong land–sea temperature contrasts (Stensrud 1996). Because the Great Plains is a region of frequent LLJ occurrence, and has historically had good data coverage by operational and research observational platforms, numerous observational studies of the LLJ have focused on that region (Lettau and Davidson 1957, Hoecker 1963, Izumi and Barad 1963, Bonner 1968, Parish *et al*. 1988, Stensrud *et al*. 1990, Mitchell *et al*. 1995, Arritt *et al*. 1997, Whiteman *et al*. 1997, Wu and Raman 1998, Walters and Winkler 2001, Banta *et al*. 2002, Song *et al*. 2005, Banta 2008, Walters *et al*. 2008, among others). The LLJ typically develops around sunset, under dry cloud-free conditions conducive to strong radiational cooling, reaches a peak intensity in the early morning hours, and then decays shortly after dawn, with the onset of daytime convective mixing. Other signature features of this phenomenon are an anticyclonic turning (veering) of the wind vector with time, and the development of a pronounced supergeostrophic southerly wind maximum (jet maximum) typically at levels less than 1 km above ground level, and frequently at levels less than 500 m above ground level. In contrast, the decrease of the wind speed with height above the jet maximum is more gradual, with the speed often attaining a local minimum value before increasing to the environmental value.

Nocturnal low-level jets exert significant and wide-ranging impacts on weather and regional climate. They provide dynamical and thermodynamical support for the development of deep convective storms and heavy rain events over the Great Plains by transporting moist air northward from the Gulf of Mexico and enhancing low-level convergence and lift (Means 1952, Pitchford and London 1962, Wallace 1975, Maddox 1980, Cotton *et al*. 1989, Augustine and Caracena 1994, Stensrud 1996, Zhong *et al*. 1996, Higgins *et al*. 1997, Arritt *et al*. 1997, Tuttle and Davis 2006). They are also efficient conveyors of lower-tropospheric air pollutants such as ozone and fine particulates, transporting pollutants hundreds of miles over the course of a night (Wilson 1978, Smith *et al*. 1978, Slinn 1982, Corsmeier *et al*. 1997, Banta *et al*. 1998, Seaman and Michelson 2000, Hardesty *et al*. 2001, Bao *et al*. 2008). The seasonal dispersal of fungi, pollens and spores, and the migration of insects, including agricultural pests and carriers of plant or animal pathogens, is also facilitated by transport in LLJs (Bourke 1970, Drake 1985, Drake and Farrow 1988, Wolf *et al.* 1990, Johnson 1995, Westbrook and Isard 1999, Wood *et al*. 2006, Zhu *et al.* 2006). Notably, the LLJ has been implicated as a preferred feeding location for Brazilian free-tailed bats in Texas due to the abundance of noctuid moths and other insects that migrate on the jet (McCracken *et al*. 2008). The strong wind shear in a LLJ is a well-known aviation hazard, especially for aircraft during takeoff or landing (Neyland 1956, Fichtl and Camp 1977, Bedard 1982, Membery 1983, Galvin

1999, Kaplan *et al*. 2000, Cole *et al*. 2000, Davies 2000, Lau and Chan 2003, Mamrosh *et al*. 2006, WMO 2007). The LLJ also has major impacts on the wind-energy industry since the enhanced winds provide a dependable source of energy but the associated shear and turbulence can damage wind-turbine rotors (Sisterson and Frenzen 1978, Eggers *et al*. 2003, Cosack *et al*. 2007, Banta *et al*. 2008, Storm *et al*. 2009). Finally, we note that the downward transport of LLJ momentum in the morning by convective turbulent mixing produces strong and gusty surface winds that can rapidly intensify wildfires (Chandler *et al*. 1991, Dentoni *et al*. 2001, Charney *et al*. 2003, Brotak 2003, Brotak and Reifsnyder 2003, NWS 2007) and generate dust storms (Wilkerson 1991, Washington *et al*. 2006, Warren *et al*. 2007).

Several theories have been advanced for the dynamical origin of LLJs. In the Blackadar (1957) theory, the nocturnal jet is described as an inertial oscillation that develops in response to the rapid stabilization of the boundary layer that occurs near sunset under relatively dry, cloud-free conditions. The process is often explained with the aid of a schematic hodograph diagram depicting the evolution of the southerly wind component v as a function of the westerly wind component u within the boundary layer, as in Fig. 1. The daytime wind represented on the hodograph by curve OAB turns

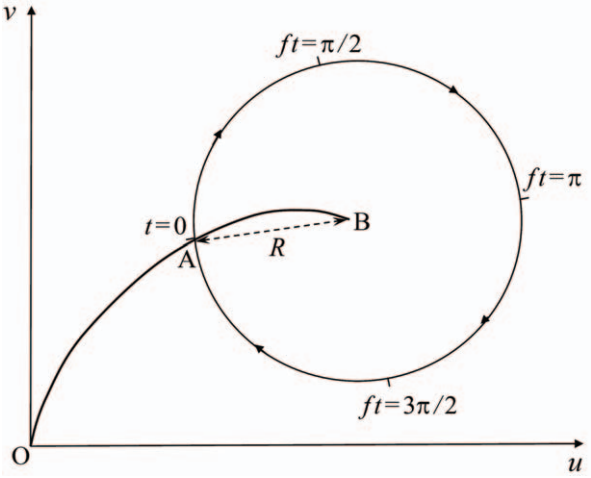

Fig. 1. Schematic of boundary-layer winds in a Northern Hemisphere inertial oscillation (adapted from Blackadar 1957). Curve OAB is the initial (t = 0) hodograph, roughly at the time of sunset. Point O is at ground level. Point B is at the top of boundary layer, where flow is considered to be geostrophic. Point A is an arbitrary location on the initial hodograph. An air parcel released from the frictional constraint at t = 0 undergoes an inertial oscillation, manifested on the hodograph plane as a circle with radius equal to the magnitude of the parcel's initial ageostrophic wind speed.

with height anticyclonically (veers) from the ground (point O) up to the top of the boundary layer (point B), where frictional effects are minimal, and the flow is nearly geostrophic (the existence of a synoptic-scale pressure gradient is a crucial component of the theory). If skies are clear and the air is dry, radiational cooling and the change of sign of the heat transfer from the ground near the time of sunset ($t = 0$) result in a rapid decay of the turbulent mixing in the boundary layer. Freed of a frictional constraint, air parcels accelerate in the direction of the pressure gradient force, and are then deflected by the Coriolis force. The post-sunset behavior of an air parcel's velocity components is described by the inviscid equations of motion, the solution of which, when drawn in the hodograph plane, is represented by a circle whose radius R is the distance of a point on the initial hodograph (e.g., point A) from the geostrophic point B. In other words, the amplitude of the oscillation (radius R) is proportional to the initial ageostrophic wind speed. Accordingly, the oscillation amplitude is expected to grow as the ground is approached until the frictional force (which is inevitably important near the ground) becomes large enough. Although not explicitly included in the Blackadar (1957) analysis, frictional stress was included in the follow-up study by Buajitti and Blackadar (1957), with the eddy viscosity varying in time and height. Thorpe and Guymer (1977), Singh *et al*. (1993) and Davies (2000) further modified this inertial-oscillation theory, mostly by considering a variety of stress parameterizations.

Although the Blackadar predictions of a LLJ hodograph that veers in time with peak winds attained in the early morning hours were confirmed qualitatively in many studies, quantitative analysis suggests that in many cases the theory may be incomplete or the considered effects may be of secondary importance. For instance, the Blackadar theory cannot explain how the peak winds in some LLJs can exceed the geostrophic values by more than 100%. Neither can it be used to explain the geographical preference of the Great Plains LLJ, namely the high frequency of LLJ formation over the sloping terrain of the Great Plains (reaching a peak around 100° W) rather than over the flatter terrain further east. In addition, reports of LLJs having a pure inertial frequency are rare. Indeed, a search for pure inertial oscillations in one month of wind profiler data from the CASES-99 field program in Kansas by Lundquist (2003) revealed that pure inertial oscillations were associated more with deformation frontogenesis accompanying frontal passages than with the evening transition of the atmospheric boundary layer (although results for frequency bands other than the pure inertial frequency were not reported). Bonner's (1968) 2-year climatological analysis also failed to turn up a latitudinal dependence to the oscillation frequency, implying the oscillation was not purely inertial.

Blackadar (1957) also suggested that there should be a close association between the height of LLJs and the vertical extent of nocturnal surface inversions. Although such an association has been reported in many studies, a large number of cases where this association was not found (e.g., Hoecker 1963, Bonner 1968, Allen 1980, Arya 1981, Mahrt *et al*. 1982, Brook 1985, Beyrich and Weill 1993, Whiteman *et al*. 1997, Milionis and Davies 2002, Hyun *et al*. 2005) suggests that a link between LLJs and surface inversions may not be straightforward. Nocturnal surface inversion layers generally increase in depth throughout the night while the height of the wind maximum can decrease, remain nearly constant, or increase with time.

A different class of theories for LLJ formation was advanced to explain the geographical preference (~100°W) of the Great Plains LLJ. Holton (1967) studied the response of the boundary layer over a sloping surface to volumetric heating represented by a function of time and height characterized by a single harmonic with a 24-hour periodicity and an e-folding depth equal to an Ekman depth based on a constant (throughout the 24-hour period) eddy viscosity. Working with the coupled viscous/diffusive boundary-layer equations and assuming a spatially and temporally constant southerly geostrophic wind, Holton showed that a diurnal wind oscillation could be induced in the sloping boundary layer by the periodic radiative forcing term. However, the results did not correctly reproduce the observed phase of the diurnal oscillations, and arguably the flow was not as jet-like as observations show. Bonner and Paegle (1970) considered a time-varying eddy viscosity and geostrophic wind, with the periodicity of the geostrophic wind ascribed to the diurnal temperature cycle over sloping terrain (although their analysis did not explicitly take terrain slope into account). Their results were in reasonable agreement with observations, but the amplitude of the oscillation was sensitive to the magnitude of the geostrophic wind, the choice of viscosity, and the phase difference between the viscosity and the geostrophic wind.

Another explanation for the geographical preference of the Great Plains LLJ relies on large-scale dynamical processes in which a latitudinal variation of the Coriolis parameter plays a key role. Wexler (1961) described the Great Plains LLJ as a northward-flowing inertial boundary layer associated with the blocking of the easterly trade winds by the Rocky Mountains, in analogy to Stommel's theory (Stommel 1958) for the westward intensification of oceanic boundary currents along eastern seaboards. Although the inertial boundary layer theory cannot explain the strong diurnal oscillation or distinctive jet-like vertical structure of the LLJ, general circulation model experiments (Ting and Wang 2006, Jiang *et al*. 2007) and regional model sensitivity experiments (Pan *et al*. 2004) indicate that a blocking mechanism is likely the dominant mechanism for maintaining the strong southerly time-mean summertime flow over the Great Plains. However, since these strong

southerly mean winds have a large geostrophic component associated with a strong westward-directed synoptic-scale pressure gradient force, the Blackadar mechanism could possibly be invoked to explain the nocturnal oscillatory behavior of the jets in that region. Thus, the Wexler mechanism (or other large-scale blocking mechanism) and the Blackadar mechanism could potentially explain different aspects of the LLJ phenomenon. However, neither of these two theories can explain the pronounced westward decrease of warm-season southerly jet frequency from 100° to 105°W evident in LLJ climatologies (Bonner 1968, Mitchell *et al*. 1995, Walters *et al*. 2008). A baroclinic theory would presumably be a likely candidate for explaining that aspect of LLJ climatology.

Although the dynamical origin of nocturnal low-level jets is still controversial, we believe that, taken collectively, the large number of published LLJ analyses makes a strong case for the LLJ arising from a force imbalance induced by the sudden release of the frictional constraint near sunset. However, the nature of the force imbalance can differ depending on a number of topographical and meteorological factors. In the case where the synoptic-scale pressure gradient force is the dominant forcing mechanism, the atmospheric response would be an inertial oscillation (Blackadar theory). However, over sloping terrain, the downslope component of the buoyancy force associated with daytime heating could also be important. In this latter case the jet could be described as an inertial-gravity oscillation rather than a pure inertial oscillation. In the present study, we systematically explore the effects of terrain slope, thermal boundary layer structure, environmental stratification and synoptic-scale pressure gradient force on LLJ evolution in as simple a framework as possible. Specifically, we extend the inviscid, one-dimensional Blackadar theory to include slope angle and a coupling between the equations of motion and thermodynamic energy. Although this approach is admittedly idealized, it leads to interesting findings concerning the possible role of terrain-associated baroclinicity in the evolution of nocturnal low-level jets.

2. PROBLEM FORMULATION AND GOVERNING EQUATIONS

Consider the development of a nocturnal low-level jet in the atmospheric boundary layer over a planar slope of infinite extent (no edge effects) having slope angle α. Our analysis proceeds in slope-following Cartesian coordinates (Fig. 2), with the x-coordinate pointing east and down the slope, and the y-coordinate pointing across the slope toward the north. We envision the jet as an oscillation induced in the boundary layer by the sudden release of a frictional constraint near sunset ($t = 0$), as in the Blackadar (1957) theory.

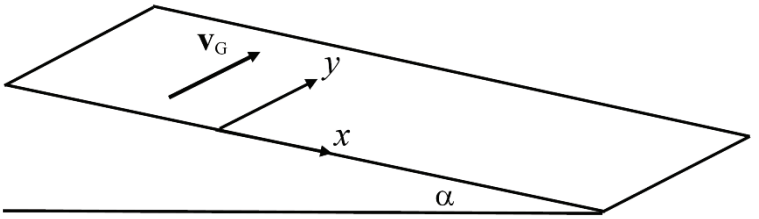

Fig. 2. Slope-following coordinate system: x is downslope coordinate, which points east (and down the slope), and y is cross-slope coordinate, which points due north. The geostrophic wind vector $\mathbf{v}_G$ is southerly (that is, it points toward the north).

However, while Blackadar proposed a purely inertial mode of oscillation, we consider a more general inertial-gravity mode of oscillation.

We restrict attention to the special case where the synoptic-scale pressure gradient force points toward the west (minus x direction), and the associated geostrophic wind is southerly ($v_G > 0$), a restriction also considered by Holton (1967).

The velocity vectors are constrained to lie within planes tangent to the slope. The corresponding coupled inviscid/non-diffusive equations of motion and thermodynamic energy are

$$\frac{\mathrm{d}u}{\mathrm{d}t} = -b\sin\alpha + fv - fv_G\,, \tag{1}$$

$$\frac{\mathrm{d}v}{\mathrm{d}t} = -fu\,, \tag{2}$$

$$\frac{\mathrm{d}b}{\mathrm{d}t} = uN^2\sin\alpha\,, \tag{3}$$

where u is the downslope velocity component, v is the cross-slope ($v > 0$ is southerly) velocity component, b is buoyancy ($b \equiv g(\theta - \theta_e)/\theta_r$, where g is the gravitational acceleration, θ is the potential temperature, θ_e is a height-varying environmental potential temperature, that is, the potential temperature in the free atmosphere, and θ_r is a constant reference potential temperature), v_G is the geostrophic wind speed, $N \equiv \sqrt{(g/\theta_r)\,\mathrm{d}\theta_e/\mathrm{d}z}$ is the free-atmosphere Brunt–Väisälä frequency, and f is the Coriolis parameter. The latter three parameters are considered constant and positive, so the geostrophic wind is constant and southerly, the free-atmosphere stratification is constant and stable, and the flow takes place in the Northern Hemisphere. It should also be born in mind that since $-fv_G$ is a proxy for the pressure gra-

dient force, the pressure gradient force is thus treated as constant. In arriving at the Coriolis terms in this coordinate system, we replaced the exact form of the slope-normal component of the Earth's angular velocity by the true vertical component. This rather mild approximation is commonly used in idealized one-dimensional models of katabatic flows with provision for the Coriolis force (see discussion and references in Shapiro and Fedorovich 2008).

So far nothing in our analysis has been implied about the local stratification, that is, the static stability within the atmospheric boundary layer. The only appearance of N in our governing equations is on the right hand side of (3), where, in combination with $\sin\alpha$, it accounts for the downslope derivative of the potential temperature. By using the free-atmosphere N in this manner, we consider the downslope derivative of potential temperature at any location within the boundary layer to be equal to the downslope derivative of potential temperature at the top of the boundary layer – and in the free atmosphere. This scenario underpins many idealized one-dimensional models of slope flows (Prandtl 1942, Gutman and Malbakhov 1964, Rao and Snodgrass 1981, McNider 1982, Sorbjan 1989, Grisogono and Oerlemans 2001, Shapiro and Fedorovich 2008 and references therein). It is depicted schematically in Fig. 6.17 of Sorbjan (1989). It is also observed over a slope in the two-dimensional numerical model simulation of McNider and Pielke (1981) in Fig. 12 (mid-afternoon) and Fig. 17 (1.5 hour before midnight). These latter two figures suggest the tilted nature of an atmospheric boundary layer that develops over a long slope. The issue of local stratification and the implications of a tilted boundary layer will be discussed later, in Section 3.

One must impose in (1)-(3) the initial values of u, v and b, that is, the values upon the release of the frictional constraint near sunset. Far above the boundary layer, the solution corresponding to $v = v_G$ (initially) is simply $v(t) = v_G$, $u(t) = 0$, and $b(t) = 0$, that is, the flow is geostrophic and neutrally buoyant at all times. Within the boundary layer, the effects of afternoon heating can be taken into account by specifying the buoyancy as an initial (sunset) condition. A positive value of buoyancy at a location within the sloping boundary layer implies that a positive potential temperature difference exists between the air at that location and the environmental air at the same elevation.

Holton (1967) considered a more general version of (1)-(3), with friction/diffusion terms and a volumetric thermal forcing term included in the thermodynamic energy equation. Although he was not concerned with a sudden release of a frictional constraint (which is central to our present considerations), his interpretation of the role of the along-slope advection of environmental potential temperature ($uN^2\sin\alpha$ in our notation) is very relevant

to our study. As discussed by Holton, this advection term generates positive buoyancy in the presence of downslope flow and negative buoyancy in the presence of up-slope flow, and thus, through the action of the downslope component of buoyancy in the downslope equation of motion, drives a tendency to oppose the down/up-slope velocity component. A similar process – the tendency for stable stratification to suppress Ekman transport on a slope – has been identified as an important process in the sloping bottom boundary layers of oceans (Thorpe 1987, Garrett 1991, MacCready and Rhines 1991, Garrett *et al*. 1993, MacCready and Rhines 1993, Ramsden 1995, Condie 1999).

3. RESULTS

Some preliminary results concerning the inertial-gravity motion are readily obtained from (2) and (3). First note that at times when $u = 0$, v and b are extrema, although at this stage we cannot say whether they are maxima or minima. Since the u wind component induces a change in v through the Coriolis term (inertial effect) as well as a proportional change in b (along-slope advection of environmental potential temperature), the changes in b and v are coupled. Using (2) to eliminate u in favor of v in (3), and integrating the result with respect to time yields

$$v N^2 \sin\alpha + b f = \text{const}. \tag{4}$$

From (4) we see that the buoyancy and southerly wind component are out of phase. Specifically, when the buoyancy is a minimum, the southerly wind component is a maximum, and *vice versa*.

Next consider the energetics of the motion. Multiplying (1) by u, (2) by $v - v_G$, and (3) by b/N^2, adding the resulting equations together, and integrating, yields

$$u^2 + \left(v - v_G\right)^2 + \frac{b^2}{N^2} = \text{const}. \tag{5}$$

Equation (5) describes a balance between the kinetic energy of the ageostrophic wind (sum of first two terms) and the potential energy associated with buoyancy.

Eliminating b between (4) and (5) yields

$$u^2 + v^2(1 + N^2 \sin^2\alpha / f^2) + m v = n,$$

where m and n are constants whose functional forms in terms of the governing parameters are rather complicated and are suppressed for the sake of clarity. This is an equation for an ellipse in the hodograph plane with major

axis directed along the u-axis (ellipse is elongated in the x-direction) and minor axis directed along the v-axis. The ratio of the major to minor axes is $\sqrt{1+N^2\sin^2\alpha/f^2}$. Interestingly, the eccentricity is independent of the geostrophic wind and of the initial values of the flow variables. In the case of flat terrain, the ellipse reduces to a circle, the familiar Blackadar result. For nonzero slope angles, the ellipse becomes more eccentric as the slope angle or stratification increase, or as the Coriolis parameter decreases.

For parameters typical of the middle portion of the central Great Plains ($\alpha \approx 0.15°$, $f \approx 8.3\times10^{-5}\text{s}^{-1}$), and N ranging from 0.01 to 0.02 s^{-1}, the ellipse is approximately 5 to 20% wider in the u-direction than in the v-direction. Results to be presented later in this section show that increased slope angle and stratification reduce the amplitude of the oscillation, with the v-component of the motion suppressed more than the u-component. An example of an elliptical hodograph generated from the analytical solution (derived below) is shown in Fig. 3 for $\alpha = 0.2°$, $f \approx 8.3\times10^{-5}\text{s}^{-1}$, and $N = 0.015$ s^{-1}. For the purpose of comparison, the circular hodograph corresponding to neutral stratification ($N = 0$) is also shown.

A predicted, west/east, elongation of LLJ hodographs is consistent with many observations over the Great Plains, for example, 4-year and 7-year average hodographs of wind deviations for July and August at Fort Worth, Texas (Fig. 14 of Bonner and Paegle 1970), a 2-year LLJ climatological

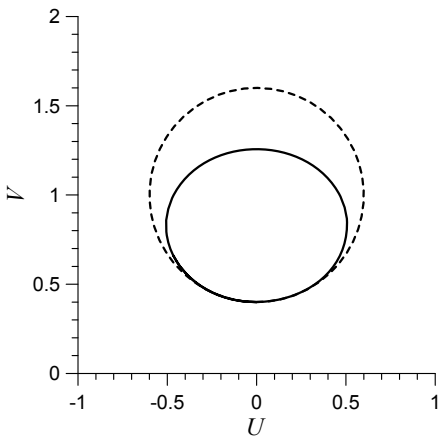

Fig. 3. Hodographs of flow oscillations over terrain at latitude 35°N ($f \approx 8.3\times10^{-5}\text{s}^{-1}$) with slope angle $\alpha = 0.2°$ for a neutrally stratified free atmosphere ($N = 0$, dashed curve) and for a stably stratified free atmosphere ($N = 0.015$ s^{-1}, solid curve). The U, and V axes represent the downslope and cross-slope wind components, respectively, normalized by the geostrophic wind speed as in (14). The two hodographs correspond to the same initial conditions: $B_0 = 0$, $U_0 = 0$, and $V_0 = 0.4$.

hodograph at a site in north-central Oklahoma (Fig. 14a of Whiteman *et al*. 1997), a 6-year LLJ climatological hodograph at a site in south-central Kansas (Fig. 8 of Song *et al*. 2005), a 2-year warm-season climatological hodograph for a site in south-east Kansas (Fig. 4 of Mitchell *et al*. 1995), and single-day hodographs for a site in north-central Nebraska (Fig. 11 of Blackadar 1957), a location over north-central Oklahoma (Fig. 5 of Parish *et al*. 1988) and several wind profiler stations over the Great Plains (Fig. 7 of Zhong *et al*. 1996). Composite hodographs of diurnal wind variations at Wichita, Kansas, and Oklahoma City, Oklahoma, for 29 days (Buajitti and Blackadar 1957) were also elliptical, but information about the absolute orientation of the ellipses was not given. At first glance, the elliptical hodograph in Fig. 18 of Bonner (1968) for 16 summer low-level jet days appears to be elongated in a more northerly direction. However, that ellipse is a subjective hand-drawn fit to four data points. The two dashed lines connecting the data points on that figure are actually more suggestive of elongation in the west/east direction.

Multiplying eq. (1) by u, eq. (2) by v, and adding the resulting equations together yields an equation for the evolution of the total kinetic energy $E_K\ [\equiv (u^2+v^2)/2]$,

$$\frac{\mathrm{d}E_{\mathrm{K}}}{\mathrm{d}t} = uF\,. \tag{6}$$

Here $F \equiv -b\sin\alpha - fv_G$ is the non-inertial part of the downslope momentum forcing, that is, the right hand side of (1) without the inertial forcing term fv. Extrema in E_K occur at times when $u = 0$ or $F = 0$. To see whether these extrema are maxima or minima, consider the second derivative of E_K, which follows from (6), (1) and (3) as

$$\frac{\mathrm{d}^2E_K}{\mathrm{d}t^2} = F\left(F + fv\right) - u^2N^2\sin^2\alpha\,. \tag{7}$$

If $F = 0$ then $\mathrm{d}^2E_K/\mathrm{d}t^2 < 0$, and the extremum is a maximum. On the other hand, if $u = 0$, the sign of $\mathrm{d}^2E_K/\mathrm{d}t^2$ depends, in general, on the sign and magnitude of the inertial forcing fv and non-inertial forcing F. However, with attention restricted to shallow slopes or large synoptic-scale pressure gradient (in the sense that F is dominated by fv_G rather than $b\sin\alpha$), the sign of $\mathrm{d}^2E_K/\mathrm{d}t^2$ is positive if $v < v_G$, and negative if $v > v_G$. Thus, if v is supergeostrophic at times when $u = 0$, the kinetic energy – and therefore v – are maximum, and b is minimum at those times. But if v is subgeostrophic when $u = 0$, the kinetic energy and v are minimum, while b is maximum.

Again, we stress that this result is only valid for inertial-gravity oscillations that behave more like inertial oscillations than gravity oscillations (that is, for very shallow slopes).

We now solve (1)-(3) explicitly. Eliminating v and b in favor of u yields

$$\frac{\mathrm{d}^2 u}{\mathrm{d}t^2} = -\omega^2 u \,, \tag{8}$$

where

$$\omega \equiv \sqrt{f^2 + N^2 \sin^2\alpha} = f\sqrt{1+\mathrm{Bu}} \,, \tag{9}$$

and $\mathrm{Bu} \equiv N^2 \sin^2\alpha / f^2$ is the slope Burger number (Garrett 1991, Garrett *et al.* 1993, Ramsden 1995). The general solution of (8) is

$$u = A\cos\omega t + D\sin\omega t \,. \tag{10}$$

Applying (10) in (2) and integrating the result yields v as

$$v = -\frac{f}{\omega}\left(A\sin\omega t - D\cos\omega t\right) + C \,. \tag{11}$$

We then obtain b as a residual from (1) as

$$b = \frac{N^2 \sin\alpha}{\omega}\left(A\sin\omega t - D\cos\omega t\right) + \frac{f}{\sin\alpha}\left(C - v_G\right) . \tag{12}$$

From (10)-(12) we see that the flow is oscillatory with a frequency ω given by (9). This is the frequency of inertial-gravity oscillations rather than of pure inertial oscillations.

Application of the initial conditions $b(0) = b_0$, $u(0) = u_0$, $v(0) = v_0$ in (10)-(12), yields A, D, C as

$$A = u_0 \,, \qquad D = \frac{1}{\omega}\left[-b_0 \sin\alpha + f\left(v_0 - v_G\right)\right],$$

$$C = \frac{N^2 \sin^2\alpha}{\omega^2} v_0 + \frac{f}{\omega^2}\left(b_0 \sin\alpha + f v_G\right) . \tag{13}$$

It is convenient to introduce the following non-dimensional variables:

$$U \equiv \frac{u}{v_G} \,, \qquad V \equiv \frac{v}{v_G} \,, \qquad B \equiv \frac{b\sin\alpha}{f v_G} \,, \qquad \Omega \equiv \frac{\omega}{f} = \sqrt{1+\mathrm{Bu}} \,,$$

$$U_0 \equiv \frac{u_0}{v_G} \,, \qquad V_0 \equiv \frac{v_0}{v_G} \,, \qquad B_0 \equiv \frac{b_0 \sin\alpha}{f v_G} \,, \qquad T \equiv f t \,. \tag{14}$$

The solution for the flow variables, expressed as deviations from initial values, then becomes

$$U(T)-U_0 = U_0\left(\cos\Omega T-1\right)+\frac{1}{\Omega}\left(-B_0+V_0-1\right)\sin\Omega T\,, \tag{15}$$

$$V(T)-V_0 = -\frac{U_0}{\Omega}\sin\Omega T+\frac{1}{\Omega^2}\left(-B_0+V_0-1\right)\left(\cos\Omega T-1\right), \tag{16}$$

$$B(T)-B_0 = \frac{\Omega^2-1}{\Omega}U_0\sin\Omega T-\frac{\Omega^2-1}{\Omega^2}\left(-B_0+V_0-1\right)\left(\cos\Omega T-1\right). \tag{17}$$

We now consider examples of flows specified by (15)-(17). Observations of boundary layers under unstable or near-neutral conditions indicate that real wind hodographs (spirals) are typically flatter than their idealized constant eddy viscosity (Ekman) counterparts, with an angle between the near-boundary velocity vector and the geostrophic wind vector typically in a range between 5° and 20°, which is much less than the Ekman model value of 45° (Zilitinkevich 1975, Hoxit 1975, Cushman-Roisin 1994). In other words, the cross-isobar wind component is typically much smaller than the geostrophic wind speed. Accordingly, we take $U_0 = 0$. For simplicity we also take $B_0 = 0$, although we will consider non-zero B_0 later. Time series of $U(T)$, $V(T)$ and $B(T)$ are shown in Fig. 4 for two subgeostrophic values of the southerly wind component, $V_0 = 0.4$ and $V_0 = 0.8$. Results will be presented for latitude 35°N ($f = 8.3\times10^{-5}\text{s}^{-1}$) with $N = 0.01$ s^{-1}, and five slope angles: 0° (Bu = 0), 0.15° (Bu = 0.1), 0.5° (Bu = 1.1), and 1° (Bu = 4.4). The Bu = 0 case corresponds to the original Blackadar (flat terrain) scenario, while the 0.15° angle characterizes the slope of the Texas and Oklahoma panhandles (around 100°W) and is close to the 1/400 slope considered by Holton (1967). The 0.5° angle is an upper bound for the slope of the High Plains of eastern Colorado and New Mexico.

The flow behavior depicted in Fig. 4 is readily explained by considering (1)-(3). Upon release of the frictional constraint, the westward-pointing pressure gradient force ($-fv_G$) is no longer fully opposed, and induces an up-slope flow ($u < 0$). Associated with this up-slope wind is a Coriolis force component ($-fu$) which increases the southerly wind component. However, the potential temperature advection associated with this up-slope wind ($u N^2 \sin\alpha$) decreases the buoyancy (so $b < 0$) and thus produces a positive downslope buoyancy force ($-b \sin\alpha$). The increasing value of the Coriolis force component fv and the increasing value of the downslope buoyancy force both oppose the pressure gradient force, and lead to a decrease in the magnitude of u, and eventually cause a reversal in the sign of u. Figure 4 also

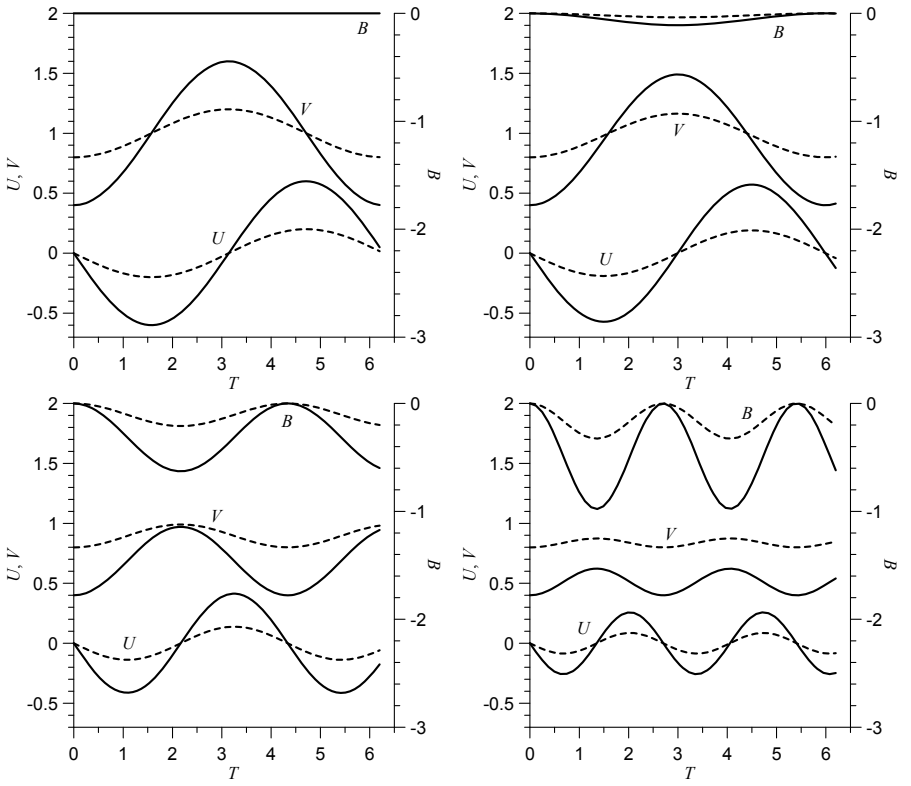

Fig 4. Time series of U, V, B at latitude 35°N with Brunt–Väisälä frequency $N = 0.01\ \mathrm{s}^{-1}$ for four slope angles: 0° (Bu = 0, upper left), 0.15° (Bu = 0.1, upper right), 0.5° (Bu = 1.1, lower left), and 1° (Bu = 4.4, lower right). Results are presented for two initial values of the southerly wind component, $V_0 = 0.4$ (solid lines) and $V_0 = 0.8$ (dashed lines). Initial values of U and B are 0. Note that the B axes are on the right side of each figure (B is negative). All plotted variables are non-dimensional.

shows that zeroes in u are associated with extrema in b and v, with maxima in v corresponding to minima in b, as was discussed above (for the parameters considered in Fig. 4, the flows are more inertial-oscillation like than gravity-oscillation like).

Continuing with the special case $U_0 = 0$, $B_0 = 0$, and the two subgeostrophic values $V_0 = 0.4$ and $V_0 = 0.8$, we consider the maximum wind speed for Bu ranging from 0 to 5. The maximum wind speed $S_{\max}$ and the time that this maximum is first obtained, $T_{\max}$, as revealed in the time series are plotted in Fig. 5. It can be shown that for the parameters considered in this plot, $S_{\max}$ corresponds to the kinetic energy maximum associated with a time when $U = 0$, so the peak southerly wind component $V_{\max}$ is equal to $S_{\max}$.

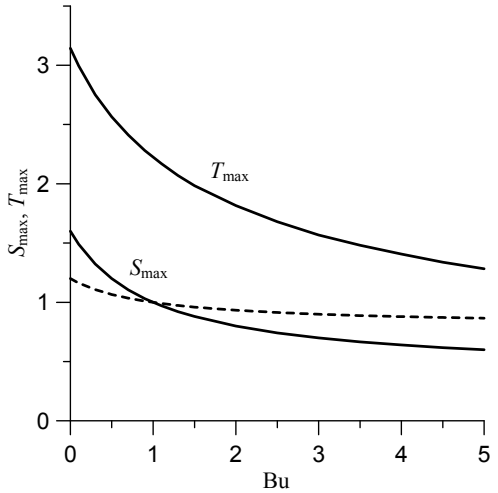

Fig. 5. Burger-number dependence of the peak wind speed S_{max} and time of peak wind speed T_{max} (= π/Ω), for two initial values of the southerly wind component, $V_0 = 0.4$ (solid line) and $V_0 = 0.8$ (dashed line). Initial values of U and B are 0. For these parameter values, the T_{max} curves corresponding to the two V_0 values are identical. All quantities are non-dimensional.

Equations (15) and (16) then reveal that the peak wind speed S_{max} first occurs at time $T_{max} = \pi/\Omega$, and is given by $S_{max} = V_0 + 2(1 - V_0)/\Omega^2$. It is convenient to rewrite this last result as

$$S_{max} = 1 + (1 - V_0) - 2(1 - V_0)\frac{\mathrm{Bu}}{1 + \mathrm{Bu}}, \qquad (U_0 = 0,\ B_0 = 0). \tag{18}$$

It is readily verified that the results in Fig. 5 agree with (18) and with the relation $T_{max} = \pi/\Omega$. In the case of Bu = 0, eq. (18) yields the Blackadar result: the peak speed is the sum of the geostrophic wind (first term, 1) and initial ageostrophic wind (second term, $1 - V_0$). For non-zero Bu, the first two terms are unaffected, and the third term is always negative (for initial winds that are subgeostrophic), which reduces the peak wind speed. For small Bu (< 1) the reduction is nearly linear in Bu, and thus nearly quadratic in the slope angle.

The Burger-number dependences of the peak wind speed and time of peak wind speed (which, for the parameter ranges considered, is related to the frequency by $T_{max} = \pi/\Omega$) are shown in Fig. 5. Regardless of Bu, larger peak speeds are associated with smaller initial values of the southerly wind component (which represent larger deviations from geostrophy), as in the Blackadar theory. But it is also clear that with steeper slopes (larger Bu) the amplitude of the oscillation is damped and the frequency is increased. The

damping is due to the generation of negative buoyancy through up-slope advection of potential temperature during the early phase of the oscillation. Associated with the negative buoyancy is a downslope buoyancy force which opposes the pressure gradient force and suppresses the oscillation. We also note that as Bu increases, v is suppressed more than u, in agreement with the previous result indicating that the major axis of the motion ellipse lies along the u-axis.

It is worth pointing out that if the late afternoon boundary layer is very well mixed then the initial wind should be a relatively large fraction of the geostrophic wind throughout much of the boundary layer, including in the area where the low-level jet would be expected to develop. In this case, the value of V_0 for parcels at the location of the jet maximum is likely closer to 0.8 than to 0.4. If the initial parcel buoyancy is very small, then using the results of Fig. 5, we see that the greatest peak jet winds to be expected would be $V_{max} = 1.2$ (corresponding to flat terrain), indicating winds that are supergeostrophic by only 20%. Moreover, peak jet winds would weaken from that relatively small value as slope angle increases. In contrast, observed peak winds in LLJs over the Great Plains can be supergeostrophic by 70% or even more, sometimes much more (e.g., Hoecker 1963, Bonner *et al*. 1968). Accordingly, if our simple framework is going to be relevant to the formation of strong low-level jets that develop within a well-mixed boundary layer over the Great Plains, initial parcel buoyancy will have to play a role.

We now consider the impact of the initial thermal structure of the boundary layer (initial values of buoyancy) on the inertial-gravity oscillation. Significantly, every appearance of B_0 and V_0 on the right hand sides of (14)-(16) is in the combination $-B_0 + V_0$. Thus, the solution for the perturbation quantities corresponding to a particular set of initial values B_{01} and V_{01} is identical to the solution corresponding to a different set, B_{02} and V_{02}, as long as these values are related by $-B_{02} + V_{02} = -B_{01} + V_{01}$. In particular, the solution corresponding to a positive initial buoyancy $B_{02} > 0$ and a particular southerly initial wind component $V_{02} > 0$ is identical to the solution with zero initial buoyancy, $B_{01} = 0$, and smaller initial wind component ($V_{01} = V_{02} - B_{02} < V_{02}$). For the parameter values considered in Figs. 4 and 5, this smaller initial wind component corresponds to a more vigorous inertial-gravity oscillation (larger initial ageostrophic wind yields a stronger oscillation). Thus, a positive initial buoyancy tends to counter the suppressive effect of the free atmosphere stable stratification. For $V_0 = 0.8$, a value of $B_0 = 0.4$ would yield the same oscillation amplitude as the case $V_0 = 0.4$, $B_0 = 0$. Considering $f = 8.3\times10^{-5}\text{s}^{-1}$, $N = 0.01\ \text{s}^{-1}$, and slope angles $\alpha = 0.15°$, 0.5°, and 1°, as in Fig. 4, and taking $v_G = 15\ \text{m s}^{-1}$, the value $B_0 = 0.4$ corresponds to rather

modest dimensional values $b_0 \approx 0.19$ m s^{-2} ($\alpha = 0.15°$), 0.057 m s^{-2} ($\alpha = 0.5°$), 0.029 m s^{-2} ($\alpha = 1°$).

We conclude this section by exploring the dependence of low level jet strength on the thermal structure of the boundary layer, and the relative location of the jet within the boundary layer. We proceed heuristically, assuming the concept of residual layer (Stull 1988) is applicable to evening transition boundary layers over terrain with small slope angles. Around the time of sunset, the layer formerly mixed by (dry) convective thermals is now characterized by weak, decaying turbulence. In the lowest portion of this layer, adjacent to the Earth's surface, a thin statically-stable boundary layer begins to develop. Above this stable boundary layer is a so-called residual layer, whose mean thermal structure is largely unchanged from its well-mixed late-afternoon state, and whose potential temperature is nearly independent of height. The residual layer extends upward to a relatively thin capping inversion (corresponding to the daytime entrainment zone) at the base of the free atmosphere. The capping inversion is typically found 1-2 km above ground level, with a strength (potential temperature jump) $\Delta\theta$ typically 1-4 K (Readings *et al*. 1973, Rayment and Readings 1974, Kaimal *et al*. 1976, Caughey and Palmer 1979, Caughey 1982, Boers and Eloranta 1986, Angevine *et al*. 1994, 1998, Cohn and Angevine 2000, Botnick and Fedorovich 2008). If we assume that a similar residual layer also develops over a slightly-inclined slope, and keep in mind that parcel buoyancy is proportional to the potential temperature difference between the parcel and the environment at the same elevation, then we are led to the notion of a tilted residual layer (TRL) that is neutrally stratified (locally) yet characterized by non-zero buoyancies. Specifically, the TRL would have a downward-directed buoyancy gradient: the layer would be positively buoyant at lower levels and negatively buoyant just beneath the capping inversion. The structure of the buoyancy field in the TRL is explained by the following analysis.

With the aid of Fig. 6, we can estimate the initial (sunset) buoyancy of an air parcel at any location within the TRL (indicated by point J). If the potential temperature is approximately constant (= θ_0) from J up to the base of the capping inversion layer, and then increases by $\Delta\theta$ across the inversion, the potential temperature at the top of the inversion at K is $\theta_0 + \Delta\theta$. The horizontal line from K to a point L in the free atmosphere is an environmental isentrope, and so the potential temperature at L is also $\theta_0 + \Delta\theta$. Since the potential temperature decreases from point L to point M (where M is in the free atmosphere location beneath point L, at the same elevation as the parcel at J) by an amount equal to the environmental potential temperature gradient $\mathrm{d}\theta_e/\mathrm{d}z$ times the altitude difference δ (> 0) between points L and M, the

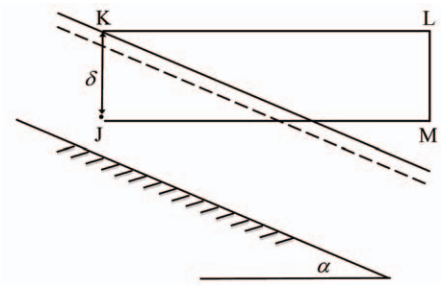

Fig. 6. Vertical cross-section through a residual layer over a shallow slope. Dashed line marks the base of the capping inversion layer. Sloping solid line passing through point K marks the top of the capping inversion layer. Symbol J marks the position of an air parcel within the residual layer, δ is the distance of the parcel from the top of the capping inversion layer, point L is in the free atmosphere at the same elevation as point K, point M is in the free atmosphere directly beneath L, at the same elevation as J. The horizontal line KL is an environmental isentrope.

potential temperature at M is $\theta_0 + \Delta\theta - \delta\, \mathrm{d}\,\theta_e/\mathrm{d}z$. Thus, the initial buoyancy for the parcel at J is $b_0 = -\mathrm{g}\Delta\theta/\theta_r + N^2\delta$, and the corresponding non-dimensional buoyancy is

$$B_0 = \frac{N^2 \sin\alpha}{f v_G}\delta - \frac{\sin\alpha}{f v_G}\frac{g\Delta\theta}{\theta_r}. \tag{19}$$

Since δ decreases with increasing slope-normal coordinate, the slope-normal derivative of B_0 (and of b_0) is negative (buoyancy decreases upward) and has a magnitude proportional to N^2, that is, it is very strongly dependent on the free-atmosphere static stability. At locations slightly beneath the capping inversion, δ is small and (19) is dominated by the second term, indicating parcels there have negative buoyancy. For parcels at sufficiently low levels, the first term dominates and the buoyancy is positive. We are especially interested in low levels because high-resolution observations of nocturnal jets indicate that the wind maximum often occurs beneath 500 m above ground level, that is, over ranges of height corresponding to the lower portion of the residual layer.

Equation (19) may shed light on an issue raised by Mahrt (1999). Since the amplitude of the classical inertial oscillation is proportional to the ageostrophic wind speed at the onset of the oscillation, and the ageostrophic wind speed in the mixed layer varies only slightly with height, one would expect a nearly uniform flow acceleration over a large part of the boundary layer, and subsequently a nearly uniform wind profile throughout the evolution of the jet, in contrast to the jet-like wind profile typically observed. However, if we make provision for sloping terrain, (19) indicates that air parcels at progres-

sively lower levels of a tilted residual layer would be associated with larger values of initial buoyancy, and as we have already demonstrated, this could induce progressively larger oscillation amplitudes.

Applying (19) in (16) at the time $T = \pi/\Omega$ when V attains a peak amplitude $V_{\max}$ (again taking $U_0 = 0$) yields

$$V_{\max} = V_0\left(1 - \frac{2f^2}{f^2 + N^2\sin^2\alpha}\right) + \frac{2f^2}{f^2 + N^2\sin^2\alpha}\left(\frac{N^2\sin\alpha}{f v_G}\delta - \frac{\sin\alpha}{f v_G}\frac{g\Delta\theta}{\theta_r} + 1\right). \tag{20}$$

From (20) we infer that the large values of $V_{\max}$ are obtained for parcels with small values of V_0 (large initial ageostrophic wind speed $1 - V_0$) located at low levels (large δ) within a residual layer with a weak capping inversion (small $\Delta\theta$).

As an example, consider $V_{\max}$ as a function of α for an air parcel at the altitude of the jet maximum with parameters typical of warm-season Great Plains low level jets: a jet maximum at 500 m above ground level with the top of the capping inversion at 1500 m above ground level (so $\delta = 1000$ m), $f \approx 8.3\times10^{-5}\,\mathrm{s}^{-1}$, $v_G = 15$ m s^{-1}, $g = 9.8$ m s^{-2}, $\theta_r = 300$ K, two values of N (0.01 s^{-1} and 0.015 s^{-1}), and five inversion strengths: $\Delta\theta = 0$, 1, 2, 3, 4 K.

Results are shown in Fig. 7 for a relatively weak initial southerly wind ($V_0 = 0.4$) and in Fig. 8 for a stronger initial wind typical of a boundary layer

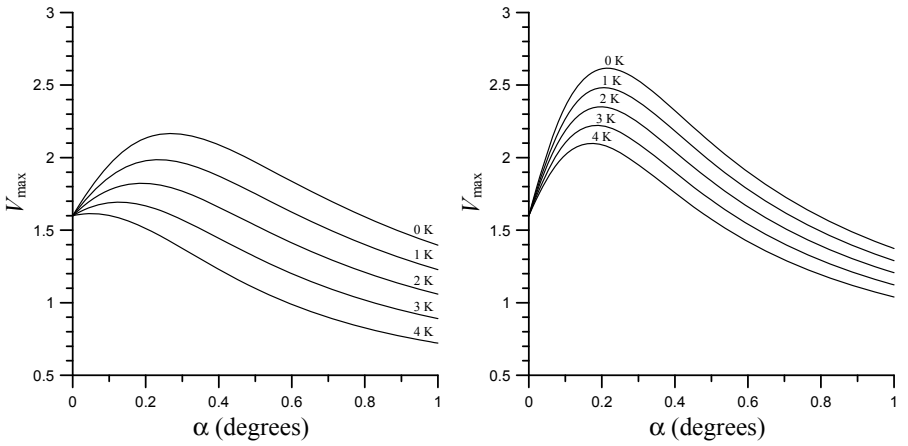

Fig. 7. Peak southerly jet speed $V_{\max}$ as a function of slope angle α for a parcel with initial southerly wind component $V_0 = 0.4$ located 1000 m beneath a capping inversion. Results are shown for five capping inversion strengths, $\Delta\theta = 0$, 1, 2, 3, 4 K, and two values of N, 0.01 s^{-1} (left panel), and 0.015 s^{-1} (right panel). See text for further details.

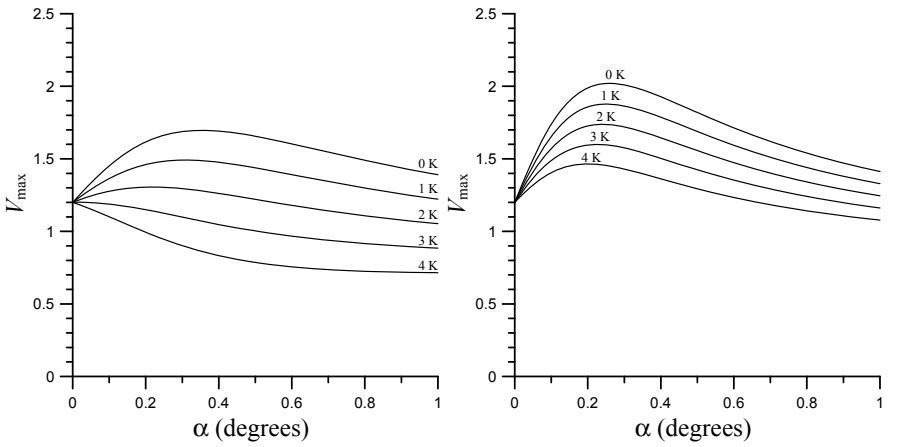

Fig. 8. As in Fig. 7 but for a parcel with initial southerly wind component $V_0 = 0.8$.

that has undergone vigorous daytime convective mixing ($V_0 = 0.8$). In most of the plotted curves, as α increases from 0º, V_{max} increases at first, and then decreases. The increase and subsequent decrease are particularly striking in the case of stronger stratification ($N = 0.015\ s^{-1}$), with peak jet winds exceeding the geostrophic winds by a factor of two. Evidently, for small α, the tendency of a positive initial buoyancy to strengthen the amplitude of the oscillation overcomes the inhibiting influence of along-slope advection of environmental potential temperature, but for the larger slope angles, advection of environmental potential temperature dominates. A simple formula for the slope angle α^* for which V_{max} is largest is obtained from $(\mathrm{d}V_{max}/\mathrm{d}\alpha)\big|_{\alpha=\alpha^*} = 0$ as

$$\alpha^* = -\frac{f v_G (1-V_0)}{N^2\delta - g\Delta\theta/\theta_r} + \sqrt{\left(\frac{f v_G (1-V_0)}{N^2\delta - g\Delta\theta/\theta_r}\right)^2 + \frac{f^2}{N^2}}\,, \tag{21}$$

where we have used the small-angle approximation $\sin\alpha^* \approx \alpha^*$.

For the parameters considered, the slope angle that maximizes the jet speed is roughly in the 0.10° to 0.20° range for $V_0 = 0.4$, and in the 0.15° to 0.25° range for $V_0 = 0.8$. A 0.15° angle characterizes the terrain slope of the central Great Plains in the longitude range 100° to 102°W; steeper slopes are found further west. The association of peak jet winds with a relatively narrow range of optimum slope angles is consistent with climatological studies that identify a longitude of maximum Great Plains LLJ frequency near 100°W (Bonner 1968, Mitchell *et al*. 1995, Walters *et al*. 2008). However, the agreement can only be regarded as qualitatively reasonable since the

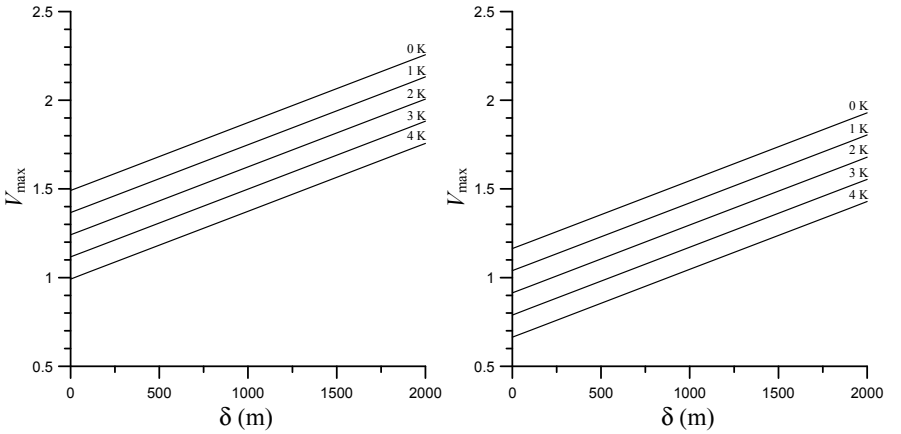

Fig. 9. Peak southerly jet speed V_{max} as a function of distance δ beneath the capping inversion for $\alpha = 0.15°$, $N = 0.01$ s^{-1} and five capping inversion strengths, $\Delta\theta = 0$, 1, 2, 3, 4 K. Results are shown for $V_0 = 0.4$ (left panel) and $V_0 = 0.8$ (right panel). See text for further details.

theoretically-optimum slope angles in the more realistic well-mixed scenario ($V_0 = 0.8$) place the optimum terrain too far to the west.

Figure 9 depicts V_{max} as a function of distance δ beneath the capping inversion for slope angle $\alpha = 0.15°$, $N = 0.01$ s^{-1}, and values of the other parameters as in Fig. 7. The presented results confirm that the larger buoyancy values at greater depths beneath the capping inversion and under conditions of weaker inversions would be associated with stronger jets.

4. SUMMARY

A simple one-dimensional inviscid model was used to study the combined effect of terrain slope, thermal boundary layer structure, environmental stratification and synoptic-scale pressure gradient on the evolution of LLJs. The scenario considered was typical of LLJs over the Great Plains of the United States: southerly geostrophic wind over terrain that slopes down toward the east. The flow is modeled as an inertial-gravity oscillation induced by the sudden release of frictional constraint near sunset, a generalization of the classical (flat-terrain) Blackadar inertial oscillation. The solution to this initial value problem was obtained analytically, and explored over a range of governing parameter values. Because of the omission of turbulent and radiative heat flux divergences, we do not expect the solution to apply within the developing shallow surface-based stable boundary layer, but only in the residual layer above it.

To identify initial (sunset) values of parcel buoyancy that might be appropriate for the Great Plains LLJ, we introduced the notion of a tilted residual layer (TRL). We assume that the residual layer around sunset is characterized by a nearly vertically-constant potential temperature, but the free atmosphere is stably stratified, and, therefore, due to the tilt of the residual layer with respect to the environmental isentropes, a vertical gradient of buoyancy exists within the residual layer. In particular, the lower part of the residual layer, where the LLJ is expected to develop, can be described as positively buoyant but locally neutrally stable. Based on the TRL concept, we obtain a simple relation for the initial parcel buoyancies in terms of terrain slope, environmental stratification, and capping inversion strength.

The free-atmosphere stratification plays two contrasting roles in our theory. On one hand, it directly inhibits the amplitude of the inertial-gravity oscillation by cooling parcels ascending along the slope and warming parcels descending along the slope (via potential temperature advection). On the other hand, it is also associated (within the TRL conceptual framework) with positive initial values of buoyancy, which result in more vigorous inertial-gravity oscillations.

Our theory yields the following predictions for the structure and behavior of the Great Plains low level jet:

- When drawn on the hodograph plain, the jet evolves as an ellipse with major axis aligned with the u-wind component. This result is consistent with observations.
- Predicted peak jet winds over flat terrain can be supergeostrophic but they are likely to be only marginally supergeostrophic. The very strongly supergeostrophic winds observed in some real jets can only be accounted for in our theory by including sloping terrain and initial parcel buoyancy (following the proposed TRL model).
- The initial (sunset) buoyancy profile within the TRL provides conditions for the flow over the slope to develop a jet-like velocity profile from a well-mixed (uniform) initial velocity field.
- The theory predicts the existence of an optimum slope angle associated with peak jet strength. This result is consistent with climatological studies of the Great Plains LLJ that identify a preferred longitude of LLJ occurrence. However, the agreement can only be regarded as qualitative, since the optimum slope angle predicted in the more realistic of our considered scenarios would be associated with terrain further west than implied by climatology.

Motivated by the generally encouraging results of the proposed theory, we will likely proceed next to numerical simulations of the early evening transition over a shallow slope under conditions typical of nocturnal jet formation. Of particular interest is the structure of the tilted residual layer and

its role in promoting jet formation, as well as the influence of friction. In view of contradictory findings on the association between the heights of surface inversions and LLJs reported in previous studies, it will also be instructive to include surface cooling, and examine the effect of the developing stable boundary layer on jet structure.

Acknowledgements. We thank Sean Arms (University of Oklahoma School of Meteorology) for kindling our interest in this subject. We are also grateful to the anonymous reviewers for their helpful comments. This research was supported in part by the United States National Science Foundation through grant ATM-0124068.

References

Allen, S. C. (1980), Observational characteristics of the low-level jet at Daly Waters during Project Koorin, *Australian Meteor. Mag*. **28**, 47-56.

Angevine, W.M., A.B. White, and S.K. Avery (1994), Boundary-layer depth and entrainment zone characterization with a boundary-layer profiler, *Bound.-Layer Meteor.* **68**, 375-385, DOI: 10.1007/BF00706797.

Angevine, W.M., A.W. Grimsdell, S.A. McKeen, and J.M. Warnock (1998), Entrainment results from the Flatland boundary layer experiments, *J. Geophys. Res.* **103,** 13689-13701, DOI: 10.1029/98JD01150.

Arritt, R.W., T.D. Rink, M. Segal, D.P. Todey, C.A. Clark, M.J. Mitchell, and K.M. Labas (1997), The Great Plains low-level jet during the warm season of 1993, *Monthly Weath. Rev*. **125**, 2176-2192, DOI: 10.1175/1520-0493 (1997)125<2176:TGPLLJ>2.0.CO;2.

Arya, S.P.S. (1981), Parameterizing the height of the stable atmospheric boundary layer, *J. Appl. Meteor*. **20**, 1192-1202.

Augustine, J.A., and F. Caracena (1994), Lower-tropospheric precursors to nocturnal MCS development over the central United States, *Weather Forecast.* **9**, 116-135, DOI: 10.1175/1520-0434(1994)009<0116:LTPTNM>2.0.CO;2.

Banta, R.M. (2008), Stable-boundary-layer regimes from the perspective of the low-level jet, *Acta Geophys*. **56**, 58-87, DOI: 10.2478/s11600-007-0049-8.

Banta, R.M., C.J. Senff, A.B. White, M. Trainer, R.T. McNider, R.J. Valente, S.D. Mayor, R.J. Alvarez, R.M. Hardesty, D. Parish, and F.C. Fehsenfeld (1998), Daytime buildup and nighttime transport of urban ozone in the boundary layer during a stagnation episode, *J. Geophys. Res*. **103**, 22519-22544, DOI: 10.1029/98JD01020.

Banta R.M., R.K. Newsom, J.K. Lundquist, Y.L. Pichugina, R.L. Coulter, and L. Mahrt (2002), Nocturnal low-level jet characteristics over Kansas during

CASES-99, *Bound.-Layer Meteor.* **105**, 221-252, DOI: 10.1023/A: 1019992330866.

Banta, R.M., Y.L. Pichugina, N.D. Kelley, B. Jonkman, and W.A. Brewer (2008), Doppler lidar measurements of the Great Plains low-level jet: Applications to wind energy, 14th International Symposium for the Advancement of Boundary Layer Remote Sensing, *IOP Conf. Series: Earth and Env. Sci.* **1**, 012020, DOI: 10.1088/1755-1307/1/1/012020.

Bao, J.W., S.A. Michelson, P.O.G. Persson, I.V. Djalalova, and J.M. Wilczak (2008), Observed and WRF-simulated low-level winds in a high-ozone episode during the Central California Ozone Study, *J. Appl. Meteor. Climatol.* **47**, 2372-2394, DOI: 10.1175/2008JAMC1822.1.

Bedard, A.J. (1982), Sources and detection of atmospheric wind shear, *AIAA J.* **20**, 940-945, DOI: 10.2514/3.51152.

Beyrich, F., and A. Weil (1993), Some aspects of determining the stable boundary layer depth from sodar data, *Bound.-Layer Meteor.* **63**, 97-116, DOI: 10. 1007/BF00705378.

Blackadar, A.K. (1957), Boundary layer wind maxima and their significance for the growth of nocturnal inversions, *Bull. Am. Meteor. Soc*. **38**, 283-290.

Boers, R., and E.W. Eloranta (1986), Lidar measurements of the atmospheric entrainment zone and the potential temperature jump across the top of the mixed layer, *Bound.-Layer Meteor*. **34**, 357-375, DOI: 10.1007/ BF00120988.

Bonner, W.D. (1968), Climatology of the low level jet, *Monthly Weath. Rev.* **96**, 833-850, DOI: 10.1175/1520-0493(1968)096<0833:COTLLJ>2.0.CO;2.

Bonner, W.D., and J. Paegle (1970), Diurnal variations in boundary layer winds over the south-central United States in summer, *Monthly Weath. Rev.* **98**, 735-744, DOI: 10.1175/1520-0493(1970)098<0735:DVIBLW>2.3.CO;2.

Bonner, W.D., S. Esbensen, and R. Greenbert (1968), Kinematics of the low-level jet, *J. Appl. Meteorol*. **7**, 339-347, DOI: 10.1175/1520-0450(1968)007< 0339:KOTLLJ>2.0.CO;2.

Botnick, A.M., and E. Fedorovich (2008), Large eddy simulation of atmospheric convective boundary layer with realistic environmental forcings. **In:** J. Meyers et al. (eds.), *Quality and Reliability of Large-Eddy Simulations*, Springer, Berlin, 193-204.

Bourke, P.M.A. (1970), Use of weather information in the prediction of plant disease epiphytotics, *Annu. Rev. Phytopathol*. **8**, 345-370, DOI: 10.1146/ annurev.py.08.090170.002021.

Brook, R.R. (1985), The Koorin nocturnal low-level jet, *Bound.-Layer Meteor*. **32**, 133-154, DOI: 10.1007/BF00120932.

Brotak, E.A. (2003), Low-level weather conditions preceding major wildfires, *Fire Management Today* **63**, 67-71.

Brotak, E.A., and W.E. Reifsnyder (2003), Predicting major wildland fire occurrence, *Fire Management Today* **63**, 20-24.

Buajitti, K., and A.K. Blackadar (1957), Theoretical studies of diurnal wind-structure variations in the planetary boundary layer, *Quart. J. Roy. Met. Soc*. **83**, 486-500, DOI: 10.1002/qj.49708335804.

Caughey, S.J. (1982), Observed characteristics of the atmospheric boundary layer, **In:** F.T.M. Nieuwstadt and H. van Dop (eds.), *Atmospheric Turbulence and Air Pollution Modelling*, D. Reidel Publishing, Dordrecht, 107-158.

Caughey, S.J., and S.G. Palmer (1979), Some aspects of turbulence structure through the depth of the convective boundary layer, *Quart. J. Roy. Met. Soc*. **105**, 811-827, DOI: 10.1002/qj.49710544606.

Chandler, C., P. Cheney, P. Thomas, L. Trabaud, and D. Williams (1991), *Fire in Forestry. Forest Fire Behavior and Effects*, Vol. 1, Krieger Publishing Company, Malabar, FL, 441 pp.

Charney, J.J, X. Bian, B.E. Potter, and W.E Heilman (2003), Low level jet impacts on fire evolution in the Mack Lake and other severe wildfires. **In:** *5th Symposium on Fire and Forest Meteorology, joint with 2nd Int. Wildland Fire Ecology and Fire Management Congress*, Am. Meteor. Soc, Orlando, FL.

Cohn, S.A., and W.M. Angevine (2000), Boundary layer height and entrainment zone thickness measured by lidars and wind-profiling radars, *J. Appl. Meteorol*. **39**, 1233-1247, DOI: 10.1175/1520-0450(2000)039<1233:BLHAEZ> 2.0.CO;2.

Cole, R.E., S.S. Allan, and D.W. Miller (2000), Vertical wind shear near airports as an aviation hazard. **In:** *9th Conference on Aviation, Range and Aerospace Meteorology*, Am. Meteor. Soc., Orlando, FL.

Condie, S.A. (1999), Ocean boundary mixing during Ekman layer arrest, *J. Phys. Oceanogr.* **29**, 2993-3001, DOI: 10.1175/1520-0485(1999)029<2993: OBMDEL> 2.0.CO;2.

Corsmeier, U., N. Kalthoff, O. Kolle, M. Kotzian, and F. Fiedler (1997), Ozone concentration jump in the stable nocturnal boundary layer during a LLJ-event, *Atmos. Environ.* **31**, 1977-1989, DOI: 10.1016/S1352-2310(96)00358-5.

Cosack, N., S. Emeis, and M. Kühn (2007), On the influence of low-level jets on energy production and loading of wind turbines. **In:** *Wind Energy: Proceedings of the Euromech Colloquium*, 325-328.

Cotton, W.R., M.S. Lin, R.L. McAnelly, and C.J. Tremback (1989), A composite model of mesoscale convective complexes, *Monthly Weath. Rev.* **117**, 765-783, DOI: 10.1175/1520-0493(1989)117<0765:ACMOMC>2.0.CO;2.

Cushman-Roisin, B. (1994), *Introduction to Geophysical Fluid Dynamics*, Prentice Hall, Englewood Cliffs, NJ, 320 pp.

Davies, P.A. (2000), Development and mechanisms of the nocturnal jet, *Meteor. Appl.* **7**, 239-246, DOI: 10.1017/S1350482700001535.

Dentoni, M.C., G.E. Defossé, J.C. Labraga, and H.F. del Valle (2001), Atmospheric and fuel conditions related to the Puerto Madryn fire of 21 January, 1994, *Meteor. Appl*. **8**, 361-370, DOI: 10.1017/S1350482701003127.

Drake, V.A. (1985), Radar observations of moths migrating in a nocturnal low-level jet, *Ecol. Entomol*. **10**, 259-265, DOI: 10.1111/j.1365-2311.1985.tb00722.x.

Drake, V.A., and R.A. Farrow (1988), The influence of atmospheric structure and motions on insect migration, *Annu. Rev. Entomol*. **33**, 183-210, DOI: 10.1146/annurev.en.33.010188.001151.

Eggers, A.J., R. Digumarthi, and K. Chaney (2003), Wind shear and turbulence effects on rotor fatigue and loads control, *J. Sol. Energy Eng*. **125**, 402-409.

Fichtl, G.H., and D.W. Camp (1977), Sources of low-level wind shear around airports, *J. Aircraft* **14**, 5-14.

Galvin, J.F.P. (1999), Forecasting for hot-air balloons and airships in the Midlands of England, *Meteor. Appl*. **6**, 351-362, 10.1017/S1350482799001292.

Garrett, C. (1991), Marginal mixing theories, *Atmos. Ocean* **29**, 313-339.

Garrett, C., P. MacCready, and P. Rhines (1993), Boundary mixing and arrested Ekman layers: rotating stratified flow near a sloping boundary, *Ann. Rev. Fluid Mech.* **25**, 291-323.

Grisogono, B., and J. Oerlemans (2001), Katabatic flow: Analytic solution for gradually varying eddy diffusivities, *J. Atmos. Sci*. **58**, 3349-3354, DOI: 10.1175/1520-0469(2001)058<3349:KFASFG>2.0.CO;2.

Gutman, L.N., and Malbakhov, V.M. (1964), On the theory of katabatic winds of Antarctic, *Met. Issled.* **9**, 150-155 (in Russian).

Hardesty, R.M., C.J. Senff, R.M. Banta, W.A. Brewer, R.J. Alvarez, L.S. Darby, and R.D. Marchbanks (2001), Lidar applications in regional air quality studies. **In:** *Geoscience and Remote Sensing Symposium, 2001. IGARSS '01. IEEE 2001 International* **3**, 1029-1031.

Higgins, R.W., Y. Yao, E.S. Yaresh, J.E. Janowiak, and K.C. Mo (1997), Influence of the Great Plains low-level jet on summertime precipitation and moisture transport over the central United States, *J. Climate* **10,** 481-507.

Hoecker, W.H. (1963), Three southerly low-level jet systems delineated by the Weather Bureau special pibal network of 1961, *Monthly Weath. Rev.* **91**, 573-582, DOI: 10.1175/1520-0493(1963)091<0573:TSLJSD>2.3.CO;2.

Holton, J.R. (1967), The diurnal boundary layer wind oscillation above sloping terrain, *Tellus* **19**, 199-205.

Hoxit, L.R. (1975), Diurnal variations in planetary boundary-layer winds over land, *Bound.-Layer Meteor*. **8**, 21-38, DOI: 10.1007/BF02579391.

Hyun, Y.-K., K.-E. Kim, and K.-J. Ha (2005), A comparison of methods to estimate the height of stable boundary layer over a temperate grassland, *Agr. Forest Meteorol.* **132**, 132-142, DOI: 10.1016/j.agrformet.2005.03.010.

Izumi, Y., and M.L. Barad (1963), Wind and temperature variations during development of a low-level jet, *J. Appl. Meteorol*. **2**, 668-673, DOI: 10.1175/1520-0450(1963)002<0668:WATVDD>2.0.CO;2.

Jiang, X., N.C. Lau, I.M. Held, and J.J. Ploshay (2007), Mechanisms of the Great Plains low-level jet as simulated in an AGCM, *J. Atmos. Sci*. **64**, 532-547, DOI: 10.1175/JAS3847.1.

Johnson, S.J. (1995), Insect migration in North America: synoptic-scale transport in a highly seasonal environment. **In:** V.A. Drake and A.G. Gatehouse (eds.), *Insect Migration: Tracking Resources through Space and Time*, University Press, Cambridge, 31-66.

Kaimal, J.C., J.C. Wyngaard, D.A. Haugen, O.R. Coté, Y. Izumi, S.J. Caughey, and C.J. Readings (1976), Turbulence structure in the convective boundary layer. *J. Atmos. Sci*. **33**, 2152-2169, DOI: 10.1175/1520-0469(1976)033 <2152:TSITCB>2.0.CO;2.

Kaplan, M.L., Y.-L. Lin, J.J. Charney, K.D. Pfeiffer, D.B. Ensley, D.S. DeCroix and R.P. Weglarz (2000), A terminal area PBL prediction system at Dallas-Fort Worth and its application in simulating diurnal PBL jets, *Bull. Am. Meteor. Soc*. **81**, 2179-2204, DOI: 10.1175/1520-0477(2000)081<2179:ATAPPS> 2.3.CO;2.

Lau, S.Y., and S.T. Chan (2003), A cresent-shaped low-level jet as observed by a Doppler radar, *Weather* **58**, 287-290, DOI: 10.1256/wea.234.02.

Lettau, H.H., and B. Davidson (eds.), (1957), *Exploring the Atmosphere's First Mile*, Vols. I and II, Pergamon Press, New York, 578 pp.

Lundquist, J.K. (2003), Intermittent and elliptical inertial oscillations in the atmospheric boundary layer, *J. Atmos. Sci*. **60**, 2661-2673, DOI: 10.1175/1520-0469(2003)060<2661:IAEIOI>2.0.CO;2.

MacCready, P., and P.B. Rhines (1991), Buoyant inhibition of Ekman transport on a slope and its effect on stratified spin-up, *J. Fluid Mech*. **223**, 631-661, DOI: 10.1017/S0022112091001581.

MacCready, P., and P.B. Rhines (1993), Slippery bottom boundary layers on a slope, *J. Phys. Oceanogr*. **23**, 5-22, DOI: 10.1175/1520-0485(1993)023<0005: SBBLOA>2.0.CO;2.

Maddox, R.A. (1980), Mesoscale convective complexes, *Bull. Am. Meteor. Soc*. **61**, 1374-1387, DOI: 10.1175/1520-0477(1980)061<1374:MCC>2.0.CO;2.

Mahrt, L., J.C. André, and R.C. Heald (1982), On the depth of the nocturnal boundary layer, *J. Appl. Meteorol*. **21**, 90-92, DOI: 10.1175/1520-0450(1982)021 <0090:OTDOTN>2.0.CO;2.

Mahrt, L. (1999), Stratified atmospheric boundary layers, *Bound.-Layer Meteor*. **90**, 375-396, DOI: 10.1023/A:1001765727956.

Mamrosh, R.D., T.S. Daniels, and W.R. Moninger (2006*),* Aviation applications of TAMDAR aircraft data reports. **In:** *12th Conf. on Aviation, Range and Aerospace Meteor.*, Am. Meteor. Soc., Atlanta, GA.

McCracken, G.F., E.H. Gillam, J.K. Westbrook, Y.-F. Lee, M.L. Jensen, and B.B. Balsley (2008), Brazilian free-tailed bats (Tadarida brasiliensis: Molossi-

dae, Chiroptera) at high altitude: links to migratory insect populations, *Integr. Comp. Biol.* **48**, 107-118, DOI: 10.1093/icb/icn033.

McNider, R.T. (1982), A note on velocity fluctuations in drainage flows, *J. Atmos. Sci.* **39**, 1658-1660, DOI: 10.1175/1520-0469(1982)039<1658:ANOVFI> 2.0.CO;2.

McNider, R.T., and R.A. Pielke (1981), Diurnal boundary-layer development over sloping terrain, *J. Atmos. Sci*. **38**, 2198-2212, DOI: 10.1175/1520-0469 (1981)038<2198:DBLDOS>2.0.CO;2.

Means, L.L. (1954), A study of the mean southerly wind-maximum in low levels associated with a period of summer precipitation in the middle west, *Bull. Am. Meteor. Soc.* **35**, 166-170.

Membery, D.A. (1983), Low level wind profiles during the Gulf Shamal, *Weather* **38**, 18-24.

Milionis, A.E., and T.D. Davies (2002), Associations between atmospheric temperature inversions and vertical wind profiles: a preliminary assessment, *Meteor. Appl*. **9**, 223-228, DOI: 10.1017/S1350482702002074.

Mitchell, M.K., R.W. Arritt, and K. Labas (1995), An hourly climatology of the summertime Great Plains low-level jet using wind profiler observations, *Weather Forecast.* **10,** 576-591, DOI: 10.1175/1520-0434(1995)010<0576: ACOTWS>2.0.CO;2.

Neyland, L.J. (1956), Change without notice, *Flying Safety* **14**, 16-20.

NWS (2007), Southeast US high fire danger weather patterns, National Weather Service Forecast Office, Jackson MS, http://www.srh.noaa.gov/jan/ SEUSFire.php

Pan, Z., M. Segal, and R.W. Arritt (2004), Role of topography in forcing low-level jets in the central United States during the 1993 flood-altered terrain simulations, *Monthly Weath. Rev.* **132**, 396-403, DOI: 10.1175/1520-0493 (2004)132<0396:ROTIFL>2.0.CO;2.

Parish, T.R., A.R. Rodi, and R.D. Clark (1988), A case study of the summertime Great Plains low level jet, *Monthly Weath. Rev.* **116**, 94-105, DOI: 10.1175/ 1520-0493(1988)116<0094:ACSOTS>2.0.CO;2.

Pitchford, K.L., and J. London (1962), The low-level jet as related to nocturnal thunderstorms over the Midwest United States, *J. Appl. Meteorol*. **1**, 43-47, DOI: 10.1175/1520-0450(1962)001<0043:TLLJAR>2.0.CO;2.

Prandtl, L. (1942), *Führer durch die Strömungslehre*, Vieweg und Sohn, Braunschweig, 382 pp. (in German).

Ramsden, D. (1995), Response of an oceanic bottom boundary layer on a slope to interior flow. Part I: Time-independent interior flow, *J. Phys. Oceanogr.* **25**, 1672-1687, DOI: 10.1175/1520-0485(1995)025<1672:ROAOBB> 2.0.CO;2.

Rao, K.S., and H.F. Snodgrass (1981), A nonstationary nocturnal drainage flow model, *Bound.-Layer Meteor*. **20**, 309-320, DOI: 10.1007/BF00121375.

Rayment, R., and C.J. Readings (1974), A case study of the structure and energetics of an inversion, *Quart. J. Roy. Met. Soc*. **100**, 221-233, DOI: 10.1002/qj.49710042409.

Readings, C.J., E. Golton, and K.A. Browning (1973), Fine-scale structure and mixing within an inversion, *Bound.-Layer Meteor*. **4**, 275-287, DOI: 10.1007/BF02265238.

Seaman, N.L., and S.A. Michelson (2000), Mesoscale meteorological structure of a high-ozone episode during the 1995 NARSTO-northeast study, *J. Appl. Meteorol*. **39**, 384-398, DOI: 10.1175/1520-0450(2000)039<0384: MMSOAH> 2.0.CO;2.

Shapiro, A., and E. Fedorovich (2008), Coriolis effects in homogeneous and inhomogeneous katabatic flows, *Quart. J. Roy. Met. Soc*. **134**, 353-370, DOI: 10.1002/qj.217.

Singh, M.P., R.T. McNider, and J.T. Lin (1993), An analytical study of diurnal wind-structure variations in the boundary layer and the low-level nocturnal jet, *Bound.-Layer Meteor*. **63**, 397-423, DOI: 10.1007/BF00705360.

Sisterson, D.L., and P. Frenzen (1978), Nocturnal boundary-layer wind maxima and the problem of wind power assessment, *Environ. Sci. Technol*. **12**, 218-221, DOI: 10.1021/es60138a014.

Slinn, W.G.N. (1982), Estimates for the long-range transport of air pollution, *Water, Air Soil Poll.* **18**, 45-64, DOI: 10.1007/BF02419402.

Smith, T.B., D.L. Blumenthal, J.A. Anderson, and A.H. Vanderpol (1978), Transport of SO_2 in power plant plumes: day and night, *Atmos. Environ.* **12**, 605-611.

Song, J., K. Liao, R.L. Coulter, and B.M. Lesht (2005), Climatology of the low-level jet at the Southern Great Plains Atmospheric Boundary Layer Experiments site, *J. Appl. Meteorol*. **44**, 1593-1606, 10.1175/JAM2294.1.

Sorbjan, Z. (1989), *Structure of the Atmospheric Boundary Layer*, Prentice Hall, Englewood Cliffs, NJ, 317 pp.

Stensrud, D.J., M.H. Jain, K.W. Howard, and R.A. Maddox (1990), Operational systems for observing the lower atmosphere: importance of data sampling and archival procedures, *J. Atmos. Oceanic Technol*. **7**, 930-937.

Stensrud, D.J. (1996), Importance of low-level jets to climate: A review, *J. Climate* **9,** 1698-1711, DOI: 10.1175/1520-0442(1996)009<1698:IOLLJT>2.0.CO;2.

Stommel, H. (1958), *The Gulf Stream*: *A Physical and Dynamical Description*, University of California Press, Berkeley, CA, 202 pp.

Storm, B., J. Dudhia, S. Basu, A. Swift, and I. Giammanco (2009), Evaluation of the Weather Research and Forecasting model on forecasting low-level jets: implications for wind energy, *Wind Energy* **12**, 81-90, DOI: 10.1002/we.288.

Stull, R.B. (1988), *An Introduction to Boundary Layer Meteorology*, Kluwer Academic Publishers, Dordrecht, 666 pp.

Thorpe, S.A. (1987), Current and temperature variability on the continental slope, *Phil. Trans. Roy. Soc. Lond. A* **323**, 471-517, DOI: 10.1098/rsta.1987.0100.

Thorpe, A.J., and T.H. Guymer (1977), The nocturnal jet, *Quart. J. Roy. Met. Soc*. **103**, 633-653, DOI: 10.1002/qj.49710343809.

Ting, M., and H. Wang (2006), The role of the North American topography on the maintenance of the Great Plains summer low-level jet, *J. Atmos. Sci*. **63**, 1056-1068, DOI: 10.1175/JAS3664.1.

Tuttle, J.D., and C.A. Davis (2006), Corridors of warm season precipitation in the central United States, *Monthly Weath. Rev.* **134**, 2297-2317, DOI: 10.1175/MWR3188.1.

Wallace, J. (1975), Diurnal variations in precipitation and thunderstorm frequency over the conterminous United States, *Monthly Weath. Rev.* **103**, 406-419, DOI: 10.1175/1520-0493(1975)103<0406:DVIPAT>2.0.CO;2.

Walters, C.K., and J.A. Winkler (2001), Airflow configurations of warm season southerly low-level wind maxima in the Great Plains. Part I: Spatial and temporal characteristics and relationship to convection, *Weather Forecast.* **16**, 513-530, DOI: 10.1175/1520-0434(2001)016<0513:ACOWSS>2.0.CO;2.

Walters, C.K., J.A. Winkler, R.P. Shadbolt, J. van Ravensway, and G.D. Bierly (2008), A long-term climatology of southerly and northerly low-level jets for the central United States, *Annals Assoc. Amer. Geog.* **98**, 521-552, DOi: 10.1080/00045600802046387.

Warren, A., A. Chappell, M.C. Todd, C. Bristow, N. Drake, S. Engelstaedter, V. Martins, S. M'bainayel, and R. Washington (2007), Dust-raising in the dustiest place on earth, *Geomorph*. **92**, 25-37, DOI: 10.1016/j.geomorph.2007.02.007.

Washington, R., M.C. Todd, S. Engelstaedter, S. M'bainayel, and F. Mitchell (2006), Dust and the low-level circulation over the Bodélé Depression, Chad: Observations from BoDEx 2005, *J. Geophys. Res*. **111**, D03201, DOI: 10.1029 /2005JD006502.

Westbrook, J.K., and S.A. Isard (1999), Atmospheric scales of biotic dispersal, *Agr. Forest Meteorol.*, **97**, 263-274, DOI: 10.1016/S0168-1923(99)00071-4.

Wexler, H. (1961), A boundary layer interpretation of the low-level jet, *Tellus* **13**, 368-378.

Whiteman, C.D., X. Bian, and S. Zhong (1997), Low-level jet climatology from enhanced rawinsonde observations at a site in the southern Great Plains, *J. Appl. Meteorol.* **36**, 1363-1376, 10.1175/1520-0450(1997)036<1363:LLJCFE>2.0.CO;2.

Wilkerson, W.D. (1991), Dust and sand forecasting in Iraq and adjoining countries, Air Weather Service Technical Note AWS/TN-01/001, Scott Air Force Base, IL, 65 pp.

Wilson, W.E. (1978), Sulfates in the atmosphere: a progress report on Project MISTT, *Atmos. Environ.* **12**, 537-547.

WMO, (2007), *Aviation Hazards*, Education and Training Programme, ETR-20. WMO/TD-No. 1390, Secretariat of the World Meteorological Organization, Geneva, Switzerland, 53 pp.

Wolf, W.W, J.K. Westbrook, J. Raulston, S.D. Pair, and S.E. Hobbs (1990), Recent airborne radar observations of migrant pests in the United States, *Phil. Trans. Roy. Soc. Lond. B* **328**, 619-630, DOI: 10.1098/rstb.1990.0132.

Wood, C.R., J.W. Chapman, D.R. Reynolds, J.F. Barlow, A.D. Smith, and I.P. Woiwod (2006), The influence of the atmospheric boundary layer on nocturnal layers of noctuids and other moths migrating over southern Britain, *Int. J. Biometeorol*. **50**, 193-204, DOI: 10.1007/s00484-005-0014-7.

Wu, Y., and S. Raman (1998), The summertime Great Plains low level jet and the effect of its origin on moisture transport, *Bound.-Layer Meteor*. **88**, 445-466, DOI: 10.1023/A:1001518302649.

Zhong, S., J.D. Fast, and X. Bian (1996), A case study of the Great Plains low-level jet using wind profiler network data and a high-resolution mesoscale model, *Monthly Weath. Rev.* **124**, 785-806, DOI: 10.1175/1520-0493(1996)124 <0785:ACSOTG>2.0.CO;2.

Zhu, M., E.B. Radcliffe, D.W. Ragsdale, I.V. MacRae, and M.W. Seeley (2006), Low-level jet streams associated with spring aphid migration and current season spread of potato viruses in the U.S. northern Great Plains, *Agr. Forest Meteorol*. **138**, 192-202, DOI: 10.1016/j.agrformet.2006.05.001.

Zilitinkevich, S.S. (1975), Resistance laws and prediction equations for the depth of the planetary boundary layer, *J. Atmos. Sci*. **32**, 741-752, DOI: 10.1175/1520-0469(1975)032<0741:RLAPEF>2.0.CO;2.

Received 1 March 2009
Accepted 11 July 2009